

# ACOUSTICS OF A SMALL ROOM : COMPARISON BETWEEN FEM AND MEASUREMENT

PC Macey      PACSYS Limited, UK  
KF Griffiths      Electroacoustic Design Ltd, UK

## 1 INTRODUCTION

Much room acoustic simulation is done using ray tracing techniques. This approach is not accurate at low frequency, as it does not model cavity modes, and is inaccurate at modelling diffraction. Similar challenges are faced by room acousticians and automotive engineers for the modally-dense low frequency part of the spectrum.

Experience of modelling the acoustics of real enclosed spaces has shown that line for line agreement of the frequency response data is not guaranteed and in fact some disagreement on the magnitude and frequency of the room modes in even simple scenarios can be expected if the boundaries of the model are assumed to be rigid.

This paper will examine the low frequency acoustics of a relatively simple room in an attempt to understand some of the effect of non-rigid boundaries. The finite element method will be used to simulate a small room excited by a sealed box subwoofer. Acoustic and vibrational measurements of the real environment will be compared to the model to explain differences, improve our understanding and drive improvements to the simulation to achieve better accuracy.

## 2 DESCRIPTION OF ROOM

The office was chosen to be a relatively simple space with simple geometry and empty of furnishings. The room was carpeted on floorboards, walls and ceiling were of painted plaster finish, and there were 2 windows, one interior and one exterior of standard residential double glazed construction. The air volume in the room is almost a perfect cuboid 2.15m x 2.5m x 2.56m, with the exclusion of the loudspeaker volume and the addition of recesses in front of the windows (partial extension in y direction). Table 1 has a list of cavity mode frequencies. It should be noted that modes 2 and 3 are close in frequency, leading to an almost degenerate mode just below 70Hz.

In making low frequency acoustical measurements, a reference source/ receiver location was chosen to be at opposite corners of the room so that all modes would be present in the resulting frequency response (M1). 3 other locations were also measured to illustrate the different frequency responses associated with the source receiver relationship.

If the room were a perfect cuboid, then each cavity mode would have a cosine variation in each of the x,y,z coordinate directions, with a non-negative number of half wavelengths. Measurement point M2, in the centre, would have zero contribution from all modes which have an odd number of half wavelengths in any of the three coordinate directions. By contrast M1, M3 and M4 will have a strong modal contribution from all modes.

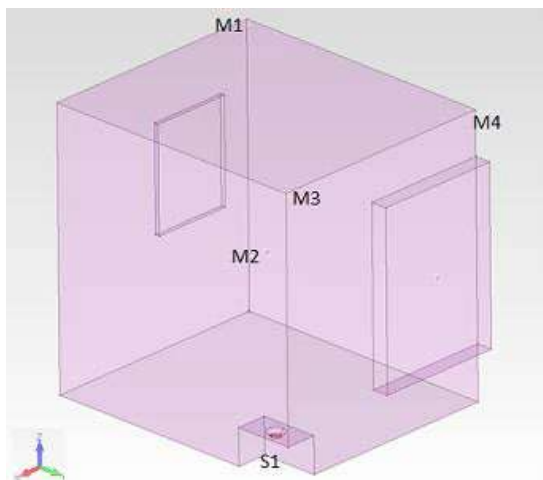


Figure 1 : position of source and microphones

mode no	frequency	description
1	0	constant pressure
2	67.118	mainly y variation
3	68.0534	mainly z variation
4	80.2739	mainly x variation
5	96.9188	yz variation
6	104.51	diag yz/x variation
7	105.91	diag yz/x variation
8	126.492	xyz variation
9	132.271	yz variation
10	136.076	yz variation
11	150.694	yz variation
12	151.998	yz variation
13	155.412	xyz variation
14	158.152	xyz variation

Table 1 : room modes

### 3 MEASUREMENT

#### 3.1 Loudspeaker Measurements

##### 3.1.1 Loudspeaker Measurements/ Definition

The loudspeaker comprised a 210mm subwoofer driver in a sealed 37.5 litre enclosure. The frequency range and anticipated signal levels meant that the loudspeaker produced sufficient output between 20Hz and 400Hz, was free of diaphragm breakup effects and did not exhibit significant nonlinear behaviour such that the parameters no longer described the loudspeaker.

The measurement of the near-field response and comparison to the frequency response of the lumped parameter model indicated good agreement up to 400Hz as seen in [8.1]. Note that there is some complementary bending of the diaphragm structure as mechanical resonance is approached at increasing frequencies resulting in the divergence of the response curves.

##### 3.1.2 Measurement of diaphragm velocity at different locations in room

In order to establish whether the room modes were affecting the loudspeaker by acoustic loading and to separate out the direct acoustic influence of the room modes, a laser Doppler vibrometer was used to obtain the diaphragm velocity which would measure only the mechanical response. The vibrometer works on the basis of 2 coherent optical beams which are split into reference and measurement beams. The measurement beam when modulated by the vibration of the test surface interferes with the reference beam and this modulation creates a frequency shift which is processed and converted to a voltage proportional to the velocity [3].

The laser measurements on the diaphragm were repeated for 2 locations in the room, the corner and centre which produce very different acoustical responses and therefore if the coupling between the room and the loudspeaker was significant, these would in turn produce different mobility responses.

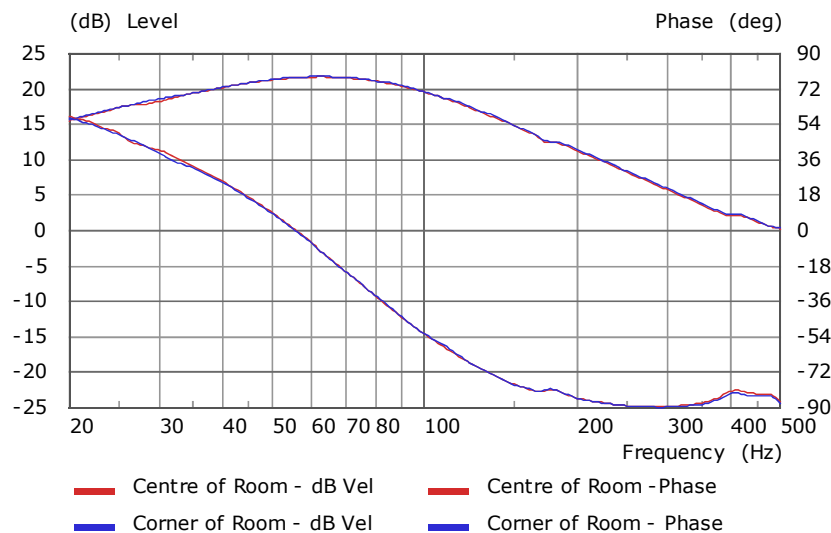


Figure 2 : measured diaphragm velocity

The phase response was also included as a second indicator on the basis that even subtle variations in the driver dynamics can be more clearly observed in this data. The comparison suggests that acoustic loading from the room has very little effect on the diaphragm velocity. This means that in this case, velocity can be prescribed without significant loss of accuracy and the problem could be run with one way coupling.

### 3.2 Frequency Response Measurements of the Room

Frequency response measurements were conducted at various microphone positions with a fixed source loudspeaker as described in section 2. The instrumentation comprised an omnidirectional pressure microphone, preamplifier and power supply connected to a computer based measurement system via an audio interface. An audio power amplifier delivered the input signal to the source loudspeaker. The system<sup>4</sup> was calibrated as necessary to produce absolute measurement of dB SPL in the test environment for a known input voltage to the loudspeaker.

The test signal used was a logarithmic chirp which was repeated 5 times to produce an average and overcome spurious noise events. An acquisition length of 128k samples was used at 48kHz with 128k FFT size to provide good resolution at low frequencies.

Structural velocity and acoustic SPL responses were acquired based on a voltage input of 1vrms applied to the loudspeaker in all measurements.

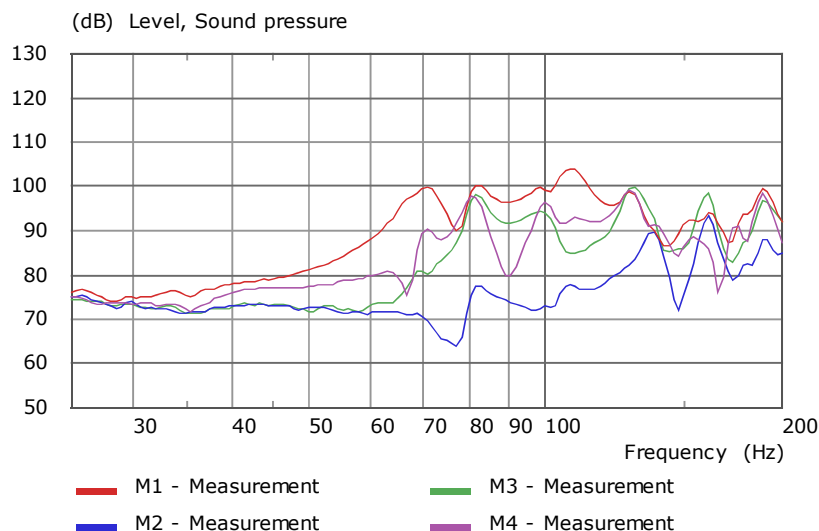


Figure 3 : measured SPL at points M1-M4

The SPL data taken from the different microphone positions show major variations as expected. Position M1, in the opposite corner to the source, results in contribution from all modes and produces the highest SPL across the band. In contrast, M2 in the centre of the room excites only even order modes for all axes and therefore significantly less reinforcement from the room modes is recorded.

With reference to the mode table in section 2, there is generally good correlation between the features in the frequency response and the theoretical eigen-frequencies computed.

### 3.3 Laser Doppler Vibrometer Measurements of the Windows

The windows were measured using the laser vibrometer and small ( $\sim 2\text{mm}^2$ ) patches of retro-reflective self-adhesive tape, attached to the glass to ensure a strong return from the vibrating surface to the sensing element of the vibrometer. Complex velocity measurements were acquired to produce a surface animation of the window. In practice, this process was not trivial and was hampered to some extent by the road noise on the opposite side of the window and the very low velocity levels involved. As a precaution, 5 swept sine measurements were taken and averaged for each point measured.

A further purpose of measuring the window in terms of the structural response was because this information could be used to help identify the material parameters and allow windows to be included in a more realistic finite element model as reactive entities. Theoretical predictions<sup>5</sup> aimed at comparing the performance of single, double and triple glazed windows have proven difficult to align with experimental results, particularly in the multiple glazed instances. The aim here will be to model the window with more realistic boundary conditions and ultimately excited by the acoustic coupling from the modal room.

In determining the properties, the idea was to consider the window initially as an acoustically uncoupled sub-system in a suitably simplified model, and then use an iterative updating approach to estimate the dynamic mechanical parameters.

#### 3.3.1 Surface Scans of Window Glass

A matrix of measurement points was defined for the window measurement as shown below.

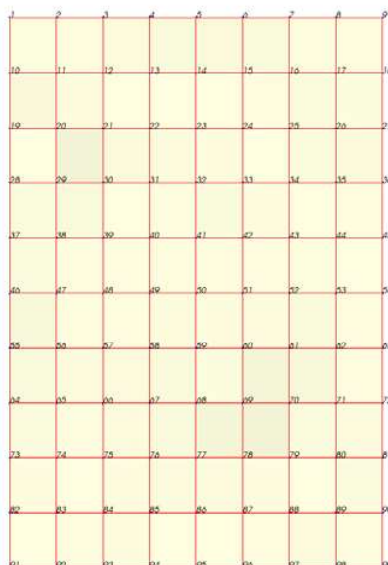


Figure 4 : measurement points on window

Initially this was rather coarse (13.45cm intervals vertically \* 11.375cm intervals horizontally), partly in anticipation of lower order mode-shapes in the windows structural response within the investigation bandwidth and also because of the effort required to perform the measurements.

The complex measurements were then combined in a special program that produced a visualisation of the moving surface within the FE modelling system. Despite efforts to reduce noise by averaging there were a number of “rogue” points that seemed to contradict the general motion displayed, however it was at least possible to identify the mode-shape of the low order modes. At higher frequencies, smaller wavelength phenomena appeared to be less comparable to the bending modes expected.

### 3.3.2 Fine Resolution Line Scan of Window Glass

In a further effort to confirm the mode-shape from the large window scan, points following the central horizontal and vertical lines of the window were measured using a finer spatial resolution of 3mm. This resolution was felt to be adequate to avoid spatial aliasing and noise allowing more confident identification of the mode-shapes.

The information provided by the laser scanning suggested that the window was moving not only in the basic mode-shapes expected of the glass pane, but had a more general pistonic and rocking behaviour superimposed. This suggested that the frame around the window was also significantly in motion. This behaviour is indicated in the images in [8.2] where the surface scan shows higher velocity at the bottom of the window and the line scans demonstrate that the edges of the glass are not stationary.

### 3.3.3 Model Updating to Estimate Window Material Parameters

Breathing modes were relatively easy to identify from the animated results as shown in [8.3]. The frequencies of these modes were noted and a window sub-system was modeled using the finite element method based on measurements of the window geometry.

The model was composed of a single pane of glass suspended in a resilient support. The actual construction of the window is presented in [8.5] where 2 panes of glass, separated by a void within which an inert gas is introduced under evacuated conditions and sealed are supported on each side by a rubber seal which is in turn mounted into a plastic window frame. The strategy for estimating the material parameters was to define the properties of the glass from literature and maintain this as a consistent property for both windows. The resilient support (usually rubber) was the “tuning” component on the basis that the practice of installing windows usually means that the outer support is subject to construction variability.

Material parameters that were plausible, applicable to both models and appeared to fit the laser animations were as follows:

Glass:  $E = 75\text{GPa}$ ,  $R_o = 2200$ ,  $Nu = 0.25$

Rubber:  $E = 0.35\text{MPa}$ ,  $R_o = 1240$ ,  $Nu = 0.4$

The resulting sub-system models are presented in appendix [8.4]. It is believed that the breathing modes are not as well formed in the experimental results due to the superposition of rocking and pistonic behaviour as the window sits as it could be seen as a mass-like entity suspended in the relatively compliant plastic outer structure of the window.

The resulting window model parameters were then applied to the model of the room to understand what effect this component would have in the coupled model.

### 3.4 Velocity Measurements of Other Surfaces

Single point measurements were additionally made at centre positions of other surfaces in the room to understand the relative contributions they may have in absorbing energy from the room.

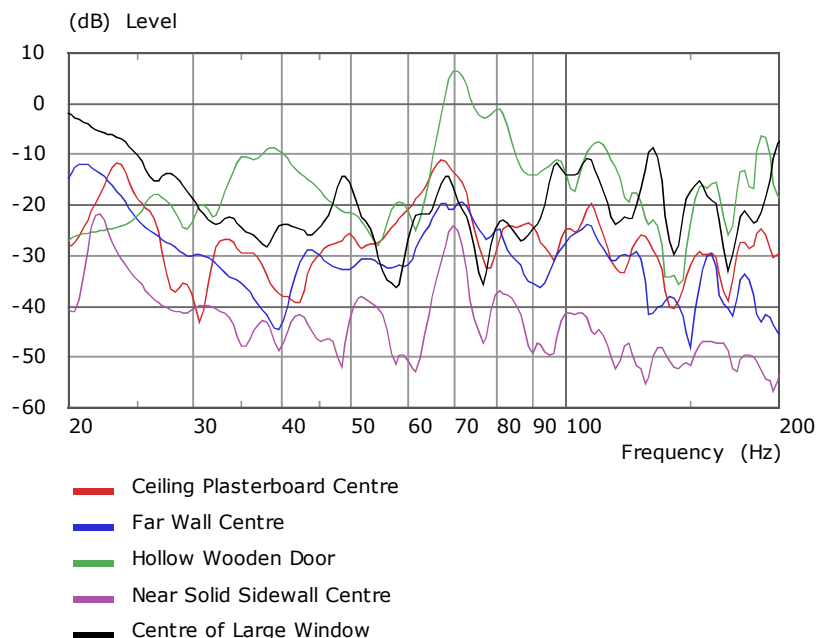


Figure 5 : measured velocity for surfaces

Although not a complete picture of the mobility of the surfaces, there is a strong indication that the entire room plays a part in absorbing sound as a resilient and potentially lossy boundary. The overall velocity level is in proportion to how lightweight the structure is – the solid wall measures

~30dB lower than the light hollow wooden door. As a point of reference, the centre of the large window sits somewhere in between. At 68 – 70Hz, the frequency of the first room mode, there is a magnification in the velocity of all the measured surfaces.

These other surfaces also occupy large areas of the room surface, considerably more than that of the windows:

**Areas in m<sup>2</sup>:**

Solid Wall: 6.216

Partition Wall: 6.400

Ceiling: 5.375

Floor: 5.218

Large Window: 1.935

Small Window: 0.735

As such, the significance of these boundaries cannot be ignored as reactive absorbing elements. It is understood from this that the acoustic energy in the room transfers into the surfaces and structure beyond, as a result is lost from the room interior reducing the magnitude of the resonance peaks measured at the microphone positions.

### **3.5 Room Measurements Investigating Basic Changes**

#### **3.5.1 Stepping the Absorption Applied to the Floor**

The carpeted floor was the only porous finish in the room, the other surfaces were painted plaster, plastic and glass or varnished wood. At frequencies below 200Hz, the wavelength of sound is much larger than the thickness of the carpet which is around 10mm. For porous absorption to be effective, it is required to be positioned in regions where the particle velocity is high. The floor however represents a boundary where particle velocity is minimal and therefore the effectiveness of the carpet as an acoustic absorber is likely to be poor. A point to note was that the floor beneath the carpet consisted of floorboards with small gaps and therefore more loss may be expected than would be the case if it were a sealed painted finish.

Measurements to compare the effect of increasing or reducing the absorbent floor layer were made. Photos of the materials involved in both scenarios to investigate this are in [8.6].

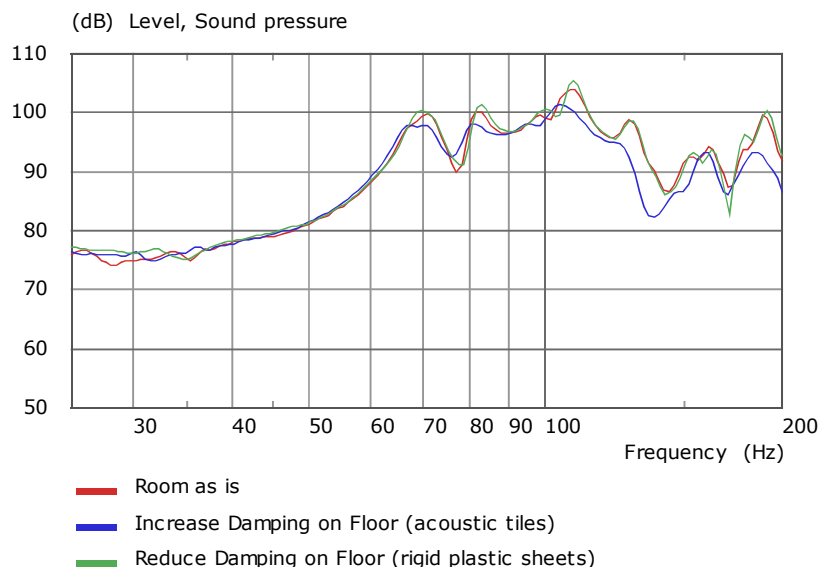


Figure 6 : Measured SPL at M1 for different floor conditions

Stepping the amount of absorption in both directions using a thicker layer of acoustic foam tiles and then a layer of hard finished plastic sheets resulted in the variations above. The addition of the hard plastic tiles made little difference to the room response, confirming that the carpet is not acoustically significant. Adding the thicker foam tiles did change the room response, lowering the magnitude and frequency of the modes.

### 3.5.2 Opening the Door

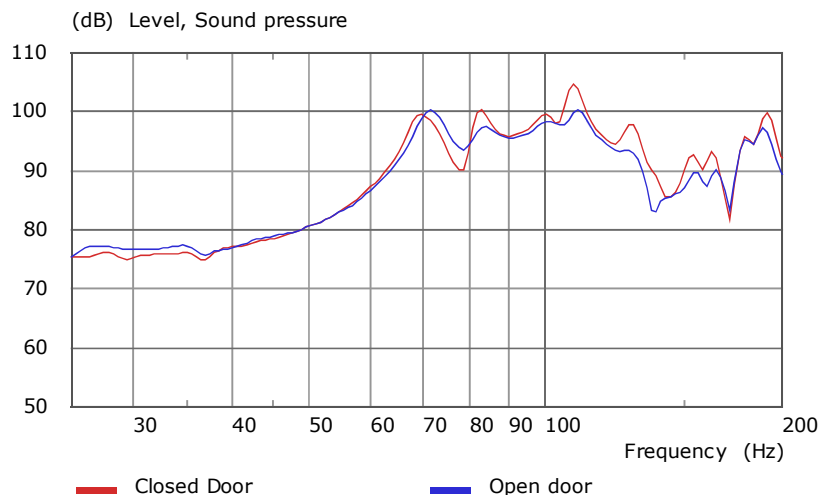


Figure 7 : measured SPL at M1 investigating effect of open door

The result of opening the door is surprisingly subtle considering the large void created in the otherwise reflective surface. The addition of foam tiles to the floor seemed to have a greater effect on overall absorption. By opening the door, the frequencies of some of the modes increase slightly



including at ~70Hz and the magnitudes reduce to reflect an increased amount of absorption in the room.

## 4 FINITE ELEMENT ANALYSIS

The room is almost a domain of constant height, i.e. with fixed cross section. Techniques<sup>1</sup> exist for doing room acoustics of such cavities rapidly, using hybrid numerical/analytical techniques. This approach was not adopted for the current work, as it would not have been possible to include the windows nor as accurate a representation of the source.

The finite element method was used to simulate the air in the room. The source could be included in a number of different ways. The simplest would be to put an ideal point source at the acoustic centre, which is not on the surface of the diaphragm, but in front, as discussed by Vanderkooy<sup>2</sup>. It is more accurate to include the enclosure, and the movement of the diaphragm. This was done on the simulation results below, prescribing the velocity measured by the laser vibrometer. This was considered to be appropriate because, as shown in the above section, the cone velocity is not affected by the room acoustics. If there were significant room/loudspeaker coupling then a different approach would have been used, modelling the mass, stiffness and damping of the driver, based on Thiele Small parameters. At higher frequencies, where cone breakup occurs, this would be insufficient, but an elastic model of the vibrating components of the driver, fully coupled to the air, could have been used.

A first attempt at modelling the small room may be to assume that the walls of the room are rigid.

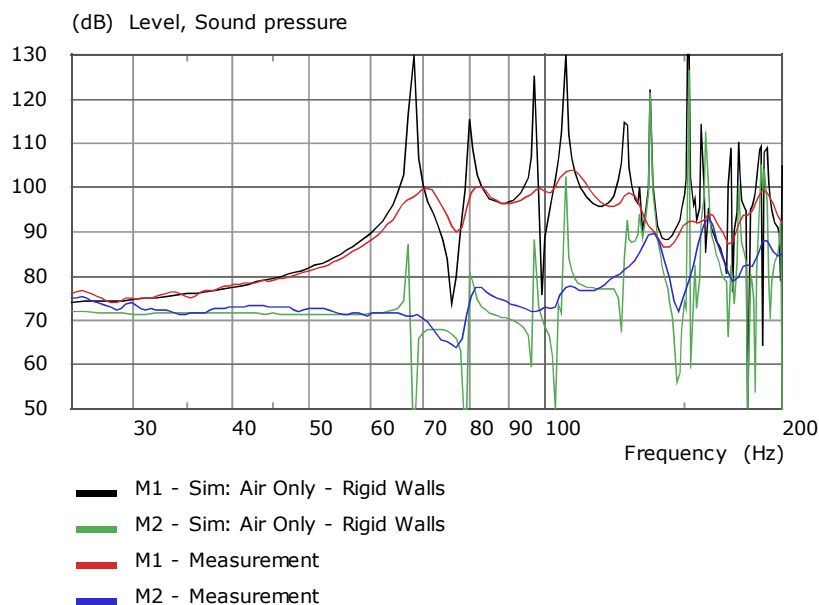


Figure 8 : SPL comparison of simulation (hard wall) and measurement

Initial observations are that the first resonance at 67Hz appears to be under-predicted in the model and there are considerably more room modes at high magnitude.

To improve the accuracy of the simulation, initially the windows were added, modelling a single plane of glass and rubber mounting, initially without damping. The air gap between panes and the exterior pane were not included in the model.

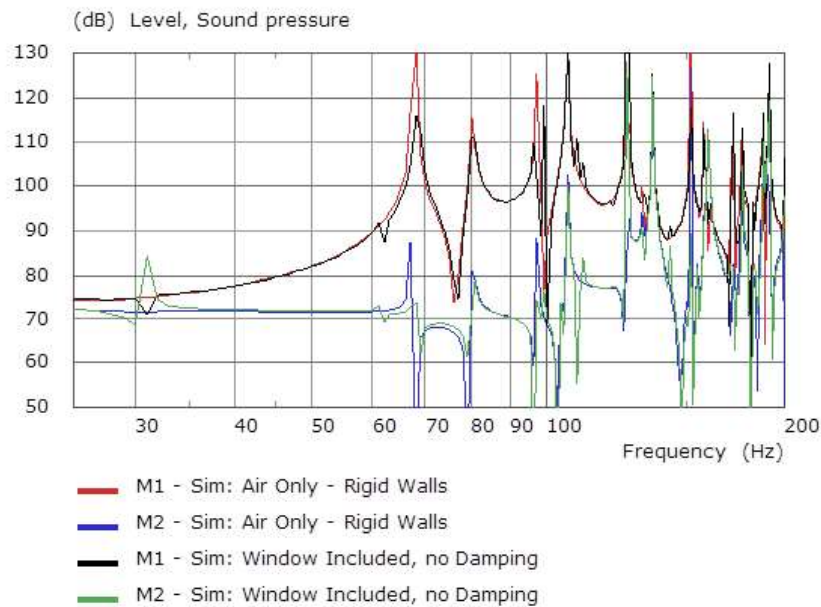


Figure 9 : effect of including undamped windows

This slightly increases the frequency of the 67Hz cavity mode resonance, certainly not up to the measured value of 70Hz. Including the structural damping in the windows mainly affects the window breathing resonances, and has little effect of acoustic cavity modes, except possibly at higher frequency..

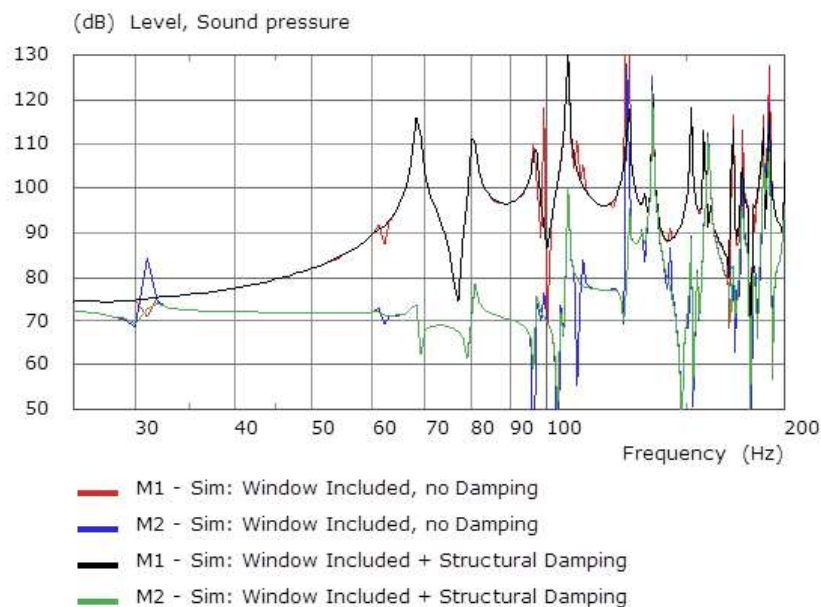


Figure 10 : effect of introducing structural damping into windows

It seems likely, particularly in view of the above velocity measurements on the other surfaces, that the majority of the damping is occurring on the door, walls, ceiling and floor. Ideally these would be modelled explicitly, but the structural material properties, thickness and points/lines of reinforcement were not known. Instead some additional damping was included as a simple acoustic impedance condition. Taking the specific acoustic impedance  $z = 10\rho c$  on floor and ceiling the damping is much more significant. All modes are damped, and some seem completely eliminated. Comparison with the measured results is much better.

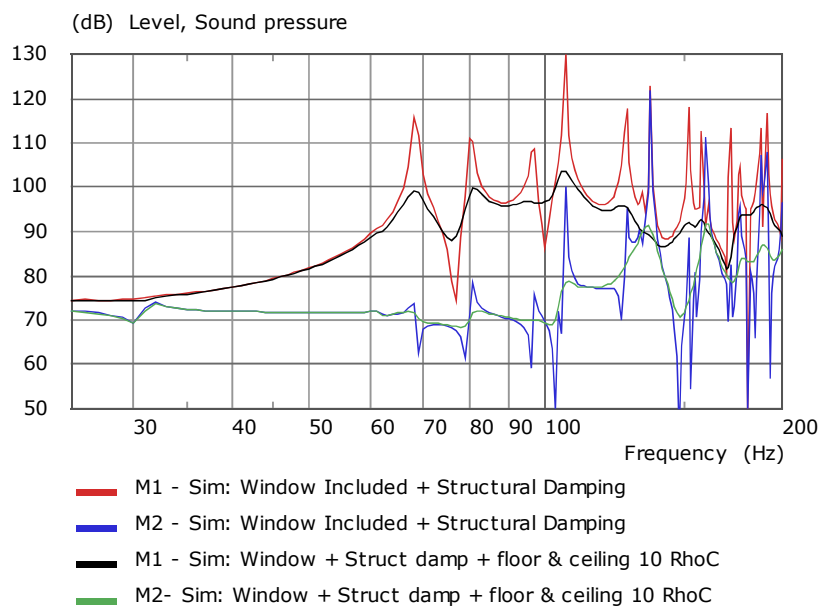


Figure 11 : effect of introducing damping on floor + ceiling

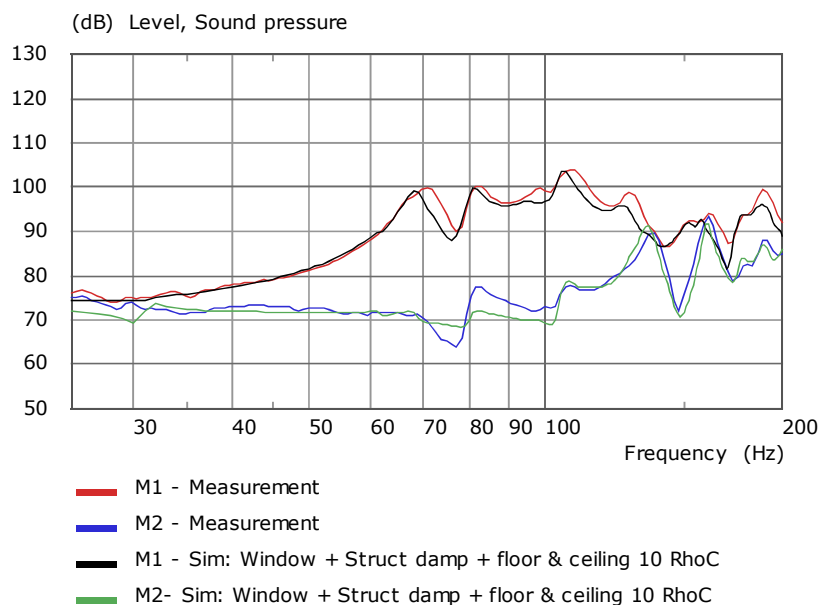


Figure 12 : SPL comparison measurement / with damped windows and floor+ceiling damping

The general damping level is about right. Similar results are obtained if the same specific acoustic impedance is put on the side (i.e. non window) walls

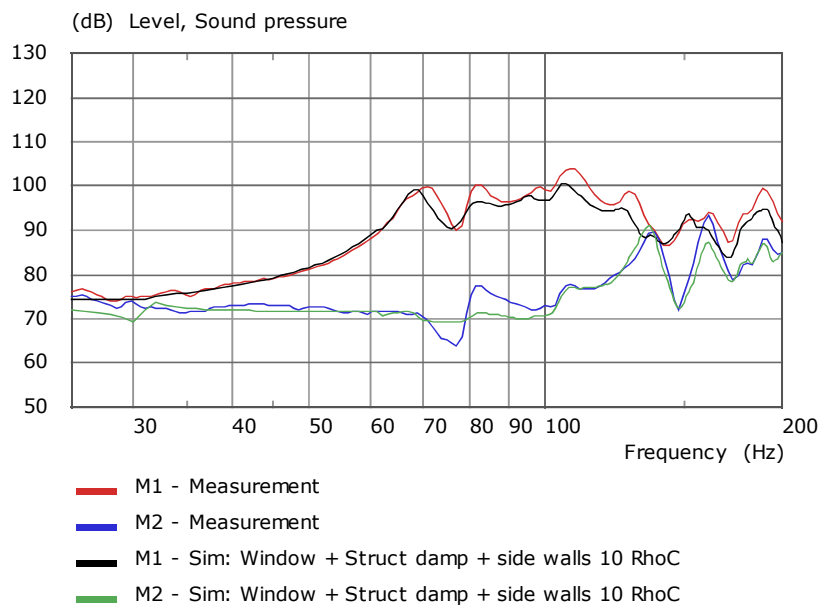


Figure 13 : SPL comparison measurement/simulation with windows and walls damping  
or a specific acoustic impedance  $z = 20\rho c$  is put on floor, ceiling and side walls.

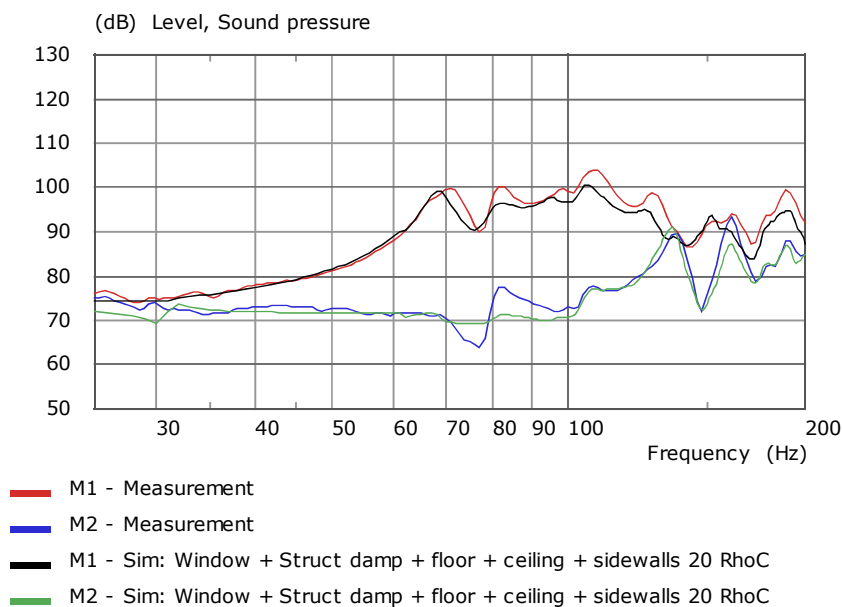


Figure 14 : SPL comparison measurement/simulation with windows and ceiling+floor+wall damping

To improve on the low frequency resonance, just below 70Hz, would require including the reactive component of the impedance on the surfaces. The best way of doing this is by a fully coupled model

with structural vibration of walls+floor+ceiling. However the details of walls, floor and ceiling are not known. Using estimates of plasterboard properties  $E=4.5 \times 10^9 \text{ N}$ ,  $\nu=0.25$ ,  $\rho=1200 \text{ kgm}^{-3}$ ,  $\tan \delta=0.3$  and assuming thickness 12.5mm on floor and walls and 9.5mm thickness for the ceiling, with stiffening at 0.5m internals, and a 20pc specific acoustic impedance on the floor, additional results were computed.

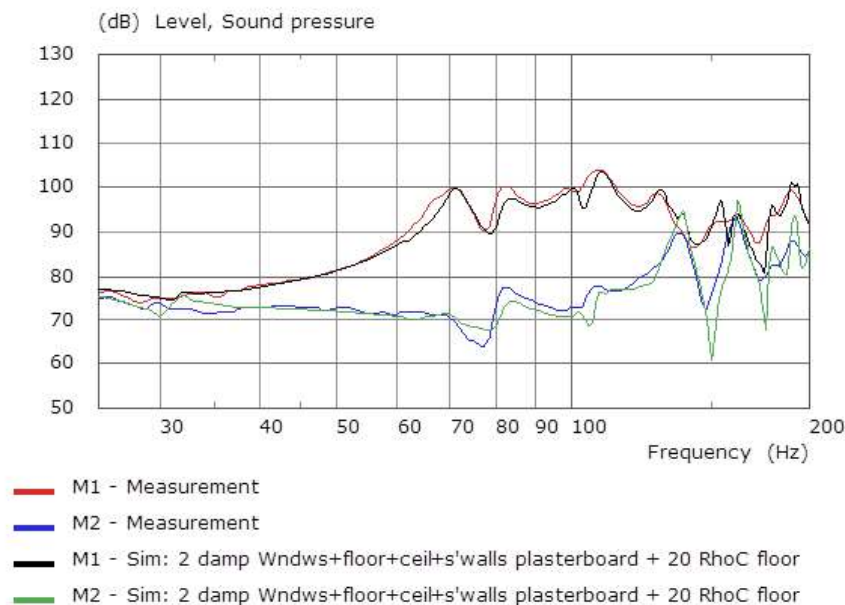


Figure 15 : comparison of SPL measurement/simulation with elastic surface representation

## 5 CONCLUSIONS

- Simulations of the room using rigid boundaries appeared to under-predict the modal frequencies, even when the geometrical definition was accurate.
- Adding a flexible window to the rigid model reduced the magnitude of the first modes and some structural resonance of the windows was evident in the room response. A slight upwards shift in the frequency of the first mode was noted, bringing it closer to the measured values. This interesting result appeared to be counter-intuitive in the sense that adding compliance to a resonant system generally reduces the frequency of the resonance.
- Including structural damping to the window and the supporting rubber did not result in a major change to the room modes, but the structural resonance that had appeared from adding the windows had diminished.
- Applying a lossy impedance condition to the floor and ceiling brought the model much closer to the measured result in terms of the overall magnitude of the room modes. This suggests that although the inclusion of the window was positive in moving the low modal frequencies higher and closer to measured values, the amount of loss was insufficient to describe the total absorption in the room possibly due to the relatively small area occupied by the windows. By increasing the floor and ceiling acoustic admittance, a more representative amount of loss resulted in a better fit with the experimental data. It is thought that the floor was particularly absorbent because underneath the carpet were floorboards presenting a rather leaky room boundary in comparison to the painted plaster finish elsewhere in the room.

- Making the floor, ceiling and sidewalls flexible as well as lossy increased the frequency of the first mode, increasing it from 68Hz to 71Hz. This behaviour was also observed to a lesser extent when the flexible windows were introduced to the model. It appears that capturing this reactive behaviour is necessary to improve the agreement between measurements and simulations. It is also possible to model this as a complex surface impedance condition (instead of a real-valued multiple of  $\rho C$ ), which may be useful because, as was encountered in this study, the precise details of the room construction may be unknown to the analyst.
- Opening the door resulted in a relatively small change in the room response. If the void created by the door could be considered to be a highly absorbent element, its inability to absorb more effectively the modes in the room suggests that the absorption area is an important factor. As was observed in the simulations with and without a realistic window model, the effect on the overall room absorption is small if the area is small.
- The laser vibrometer measurements showed that the window frame beyond the rubber seals was in motion, resulting in a super-imposed piston and rocking behaviour which was not modelled. This made a straightforward comparison of structural modes in the window difficult in addition to the challenge of recovering consistent and clean velocity data from the effects of extraneous noise.

## 6 ACKNOWLEDGEMENTS

The authors would like to acknowledge assistance from John King of PACSYS Limited, who setup many of the finite element models.

All FEM computations were done using the PAFEC VibroAcoustics program.

## 7 REFERENCES

1. Macey, P. "Room Acoustic Analysis using a 2.5 Dimensional Approach", Proc IoA Vol 33 Pt 6, Nov 2011
2. Vanderkooy, J. (2010). The low-frequency acoustic centre: Measurement, theory and application. 128th Audio Engineering Society Convention 2010
3. Basic Principles of Vibrometry, <http://www.polytec.com/uk/solutions/vibration-measurement/basic-principles-of-vibrometry/>
4. Mateljan Ivo, ARTA user manual, 2004 - 2015
5. Antonio J.B. Tadeu, Diogo M.R. Mateus, "Sound transmission through single, double and triple glazing. Experimental evaluation", Applied Acoustic 62, 2001

## 8 APPENDICES

### 8.1 Lumped Parameters and Near-field Measurement of Loudspeaker

Thiele-Small Parameters		
Fs	51.81	Hz
Re	3.9	ohms[dc]
Qt	0.64	-
Qes	0.69	-
Qms	8.76	-
Mms	60.05	grams
Rms	2.231219	kg/s
Cms	0.000157	m/N
Vas	9.38	liters
Sd	206.12	cm <sup>2</sup>
Bl	10.539264	Tm
ETA	0.18	%
Lp(2.83V/1m)	87.84	dB
Le	504.84	uH
L2	1099.58	uH
R2	27.81	ohms
L3	0	uH
R3	0	ohms



Table 2 : Thiele Small parameters

Figure 16 : near field measurement setup

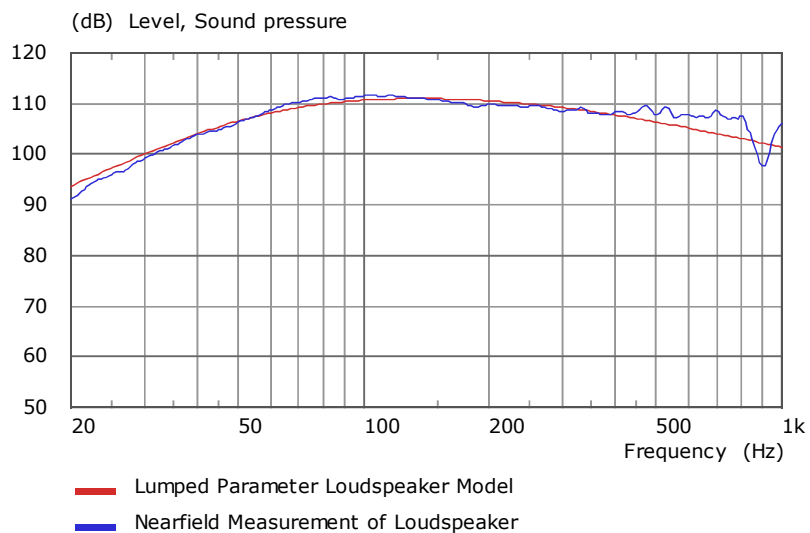


Figure 17 : comparison of lumped parameter and measurement

## 8.2 Laser Doppler Vibrometer Scan Output at 70Hz

### 8.2.1 Surface Scan of Large Window

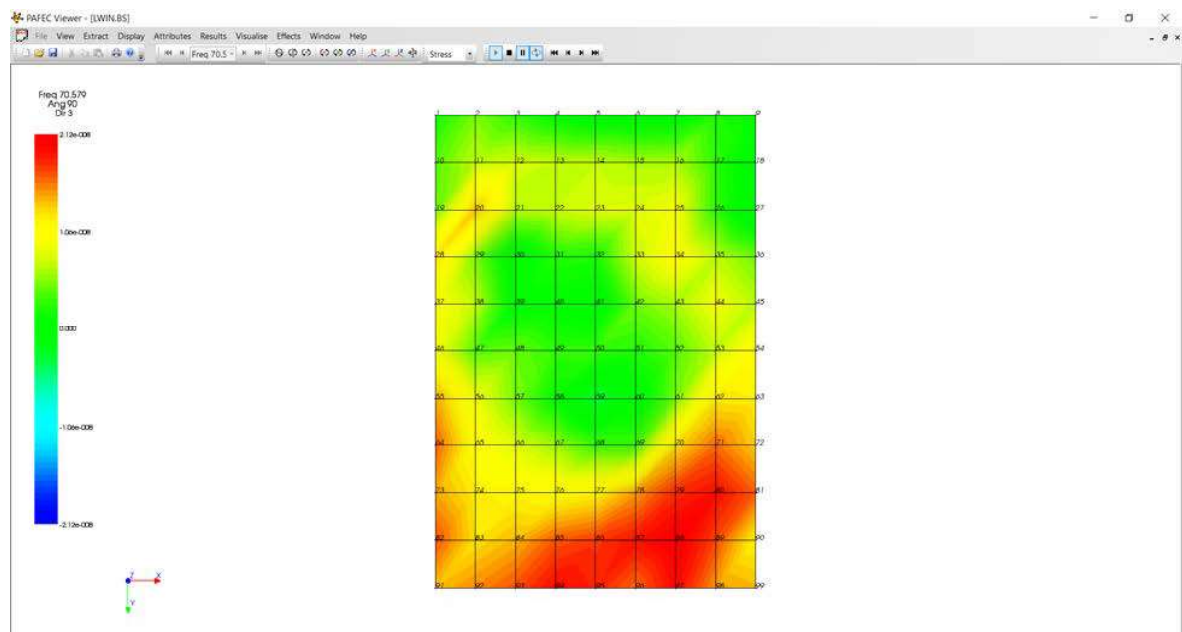


Figure 18 : vibration distribution from window scan

### 8.2.2 Horizontal Line Scan

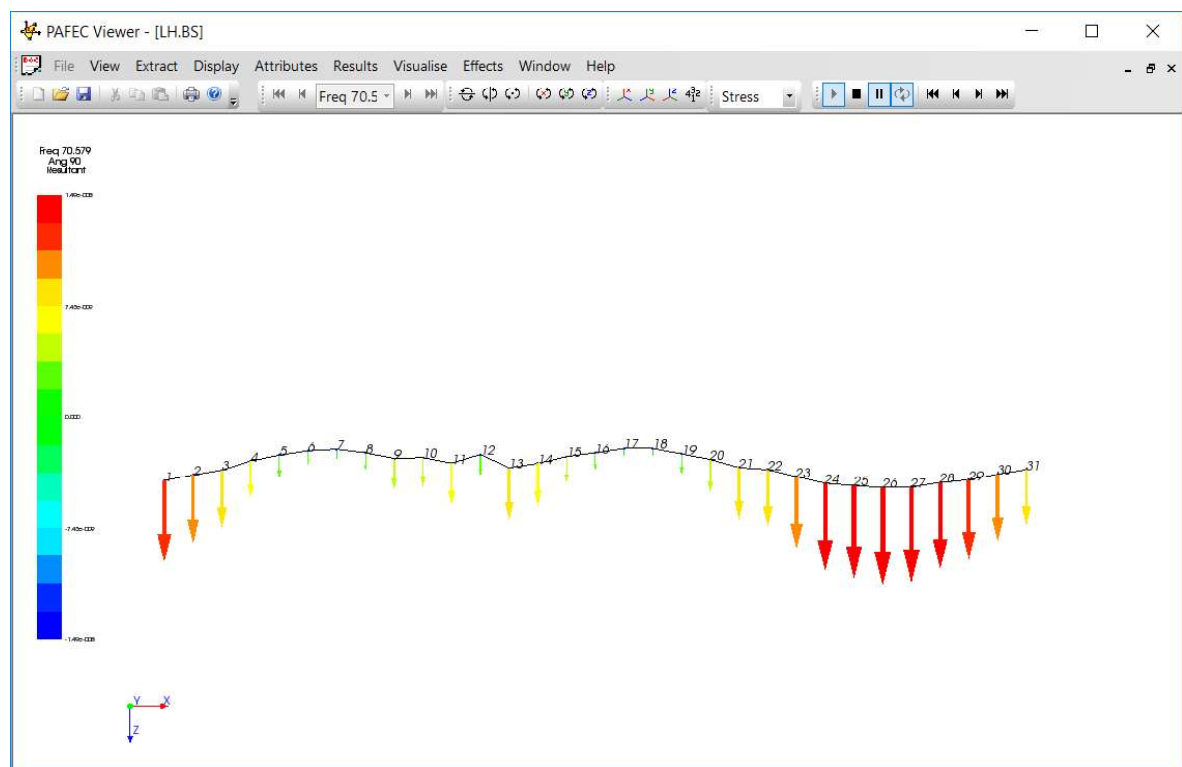


Figure 19 : vibration on horizontal line scan of window



### 8.2.3 Vertical Line Scan

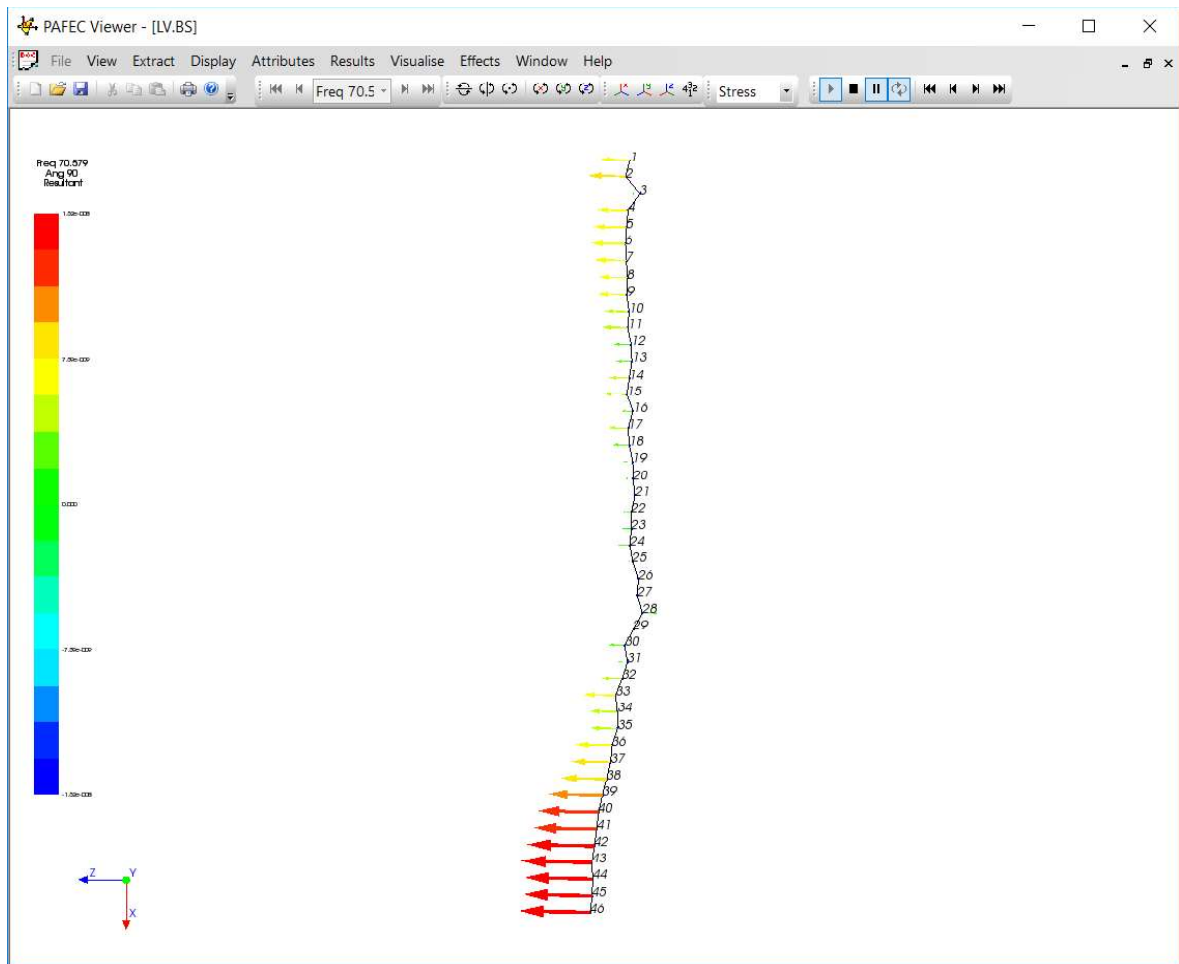


Figure 20 : vertical line scan on window

## 8.3 Measurement and Models to Estimate Material Parameters for the Window Sub-System

### 8.3.1 Large Window: Breathing mode 20Hz

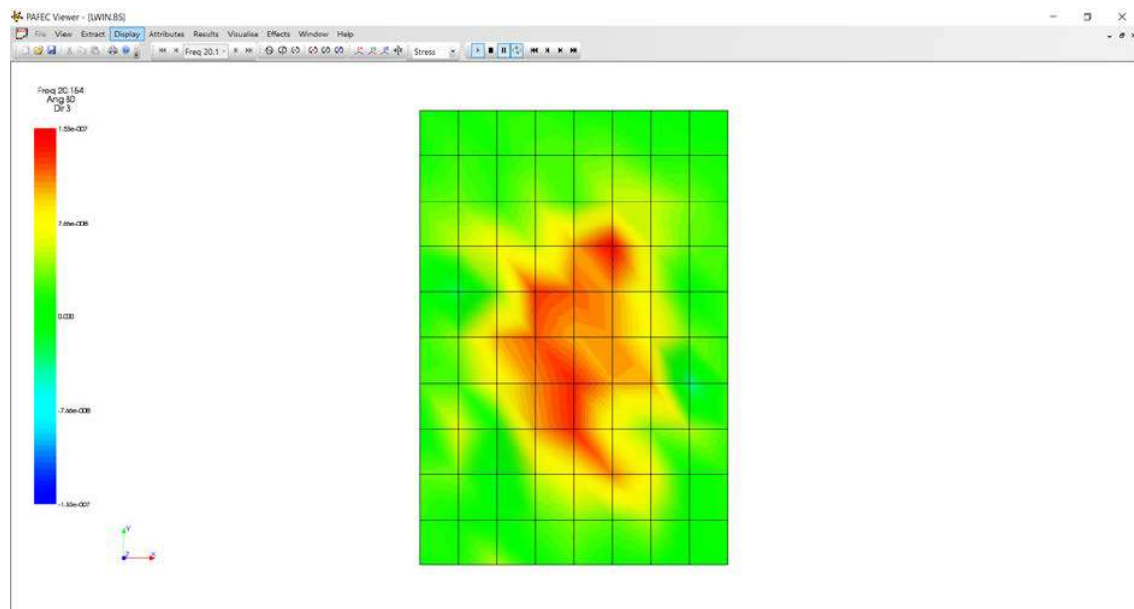


Figure 21

### 8.3.2 Small Window: Breathing mode 27Hz

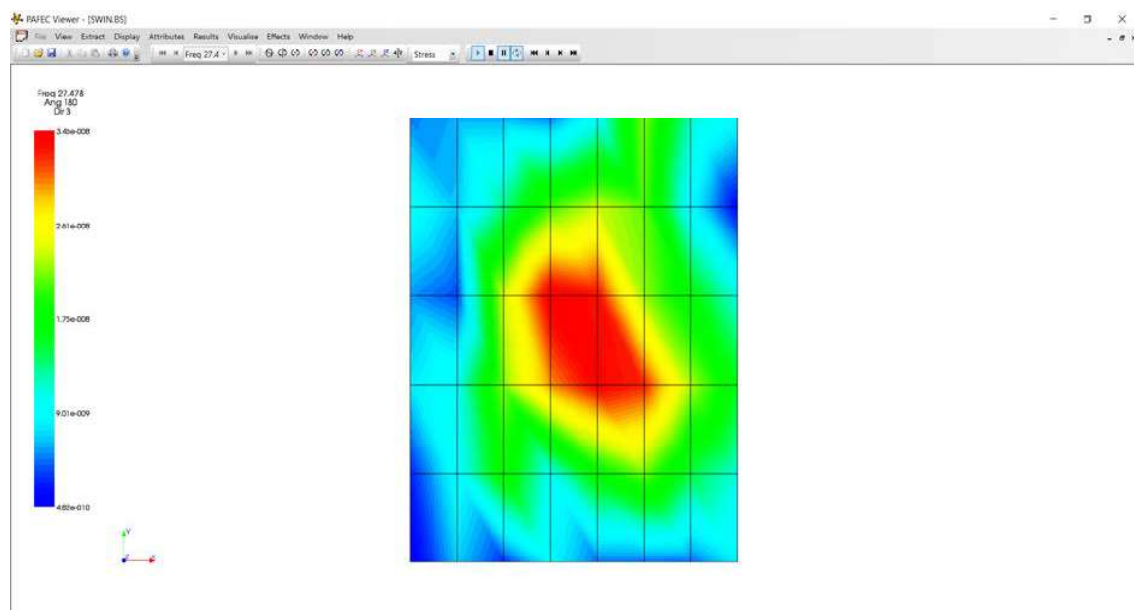


Figure 22

## 8.4 Material Identification of Windows

### 8.4.1 Large Window: Breathing mode 18Hz

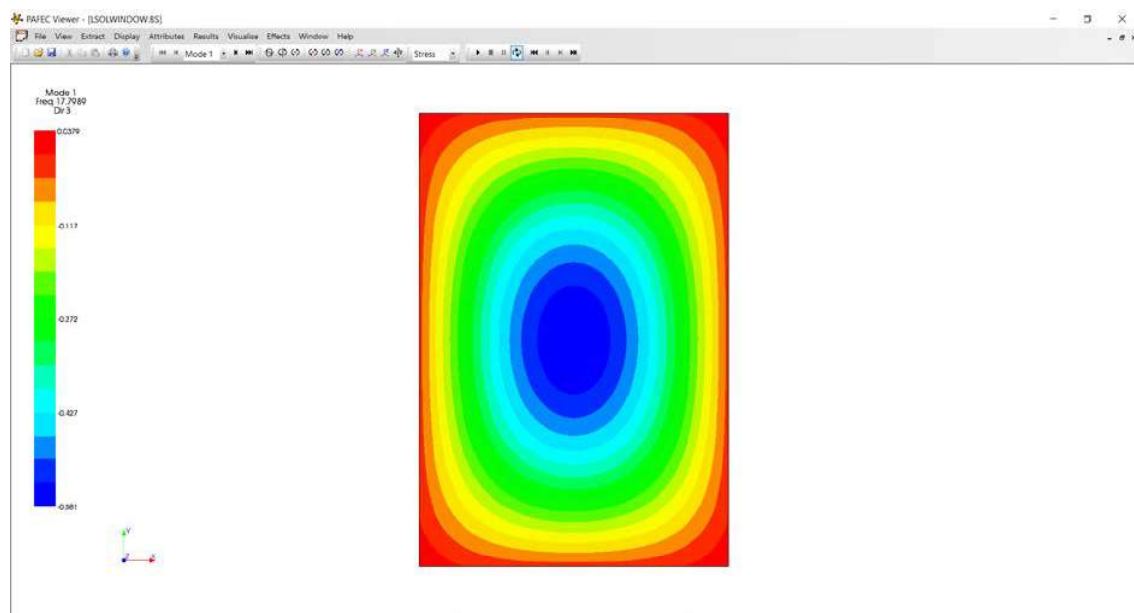


Figure 23

### 8.4.2 Small Window: Breathing mode 30Hz

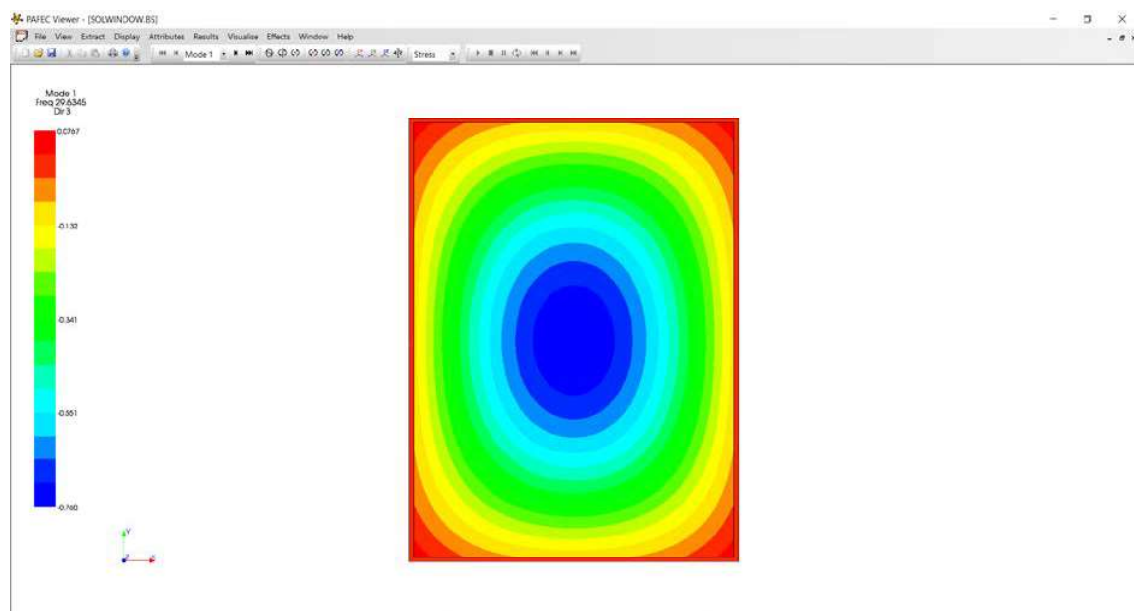


Figure 24

## 8.5 Details of Window Construction

### 8.5.1 Diagram Showing Measured Sectional Details

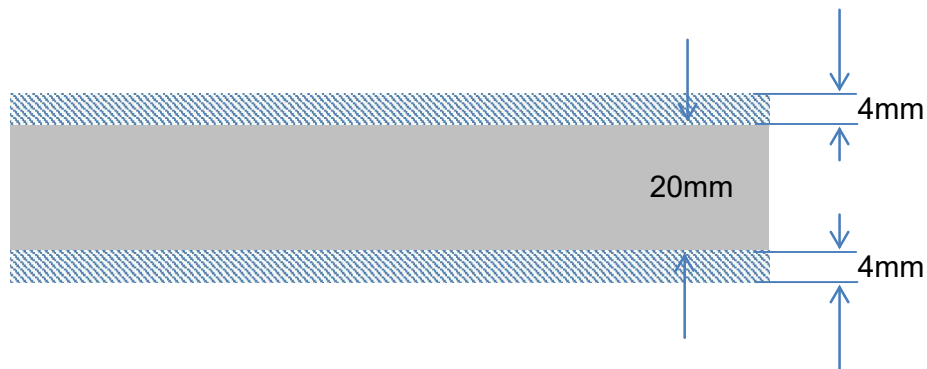


Figure 25

### 8.5.2 Photos of a Double Glazed Window Sectional Detail



Figure 26

## 8.6 Different Finishes Applied to Floor

### 8.6.1 Absorbent Tiles Laid Over Carpeted Floor



Figure 27

### 8.6.2 Hard Plastic Tiles Covering Carpeted Floor



Figure 28